Supporting information: Plasma-based dry reforming of methane in a dielectric barrier discharge reactor: Importance of uniform (sub)micron packing/catalysts to enhance the performance

Jinxin Wang[a,b,1], Kaimin Zhang[b,1], Myrjam Mertens[c], Annemie Bogaerts[a]* and Vera Meynen[b,c]*

[a]Plasma Lab for Applications in Sustainability and Medicine - ANTwerp, Department of Chemistry, University of Antwerp, Universiteitsplein 1, 2610 Wilrijk, Antwerp, Belgium

[b]Laboratory of Adsorption and Catalysis, Department of Chemistry, University of Antwerp, Universiteitsplein 1, 2610 Wilrijk, Antwerp, Belgium

[c]Flemish Institute for technological research, VITO NV, Boeretang 200, 2400 Mol, Belgium

*Email: vera.meynen@uantwerpen.be; annemie.bogaerts@uantwerpen.be

[1]These authors contributed equally to this work.

Due to the presence of systematic errors in gas components for GC analysis caused by gas expansion of DRM, 10 mL/min of N_2 was added into the outlet gas (without passing through the reactor) as an internal standard to correct the measurements. For example, the $CH_{4,out}$ was corrected from the measured value $CH_{4,out,m}$ by the following equations:

$$CH_{4,out} = CH_{4,out,m}(1 + \frac{\alpha}{\beta}) \quad \text{(S1)}$$

$$\alpha = \frac{N_{2,b}}{N_{2,p}}(1 + \beta) - \beta \quad \text{(S2)}$$

$$\beta = \frac{N_{2,b}}{CH_{4,in} + CO_{2,in}} \quad \text{(S3)}$$

Where $N_{2,b}$ and $N_{2,out}$ are the amount of N_2 measured by GC before and after starting plasma, respectively.

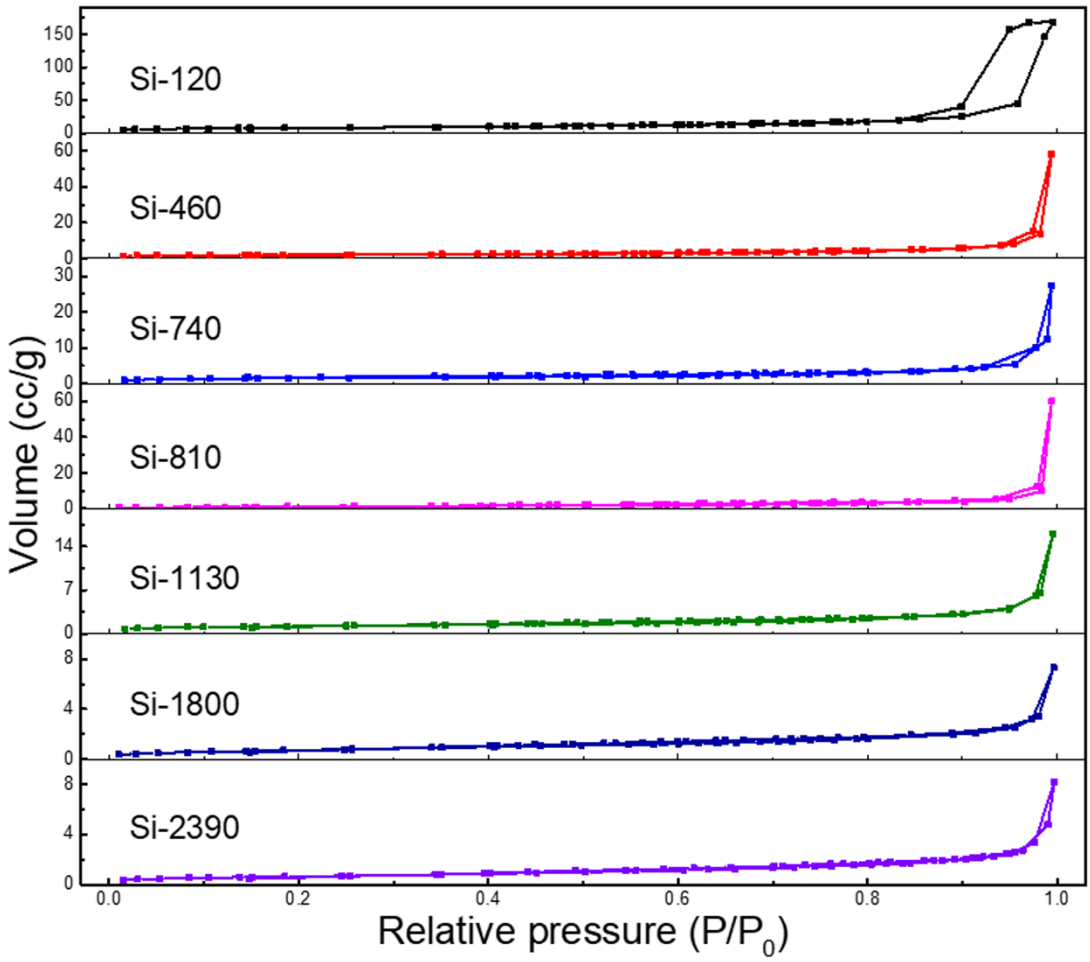

Figure S1. The N_2-sorption isotherms of SiO_2 with different particle sizes.

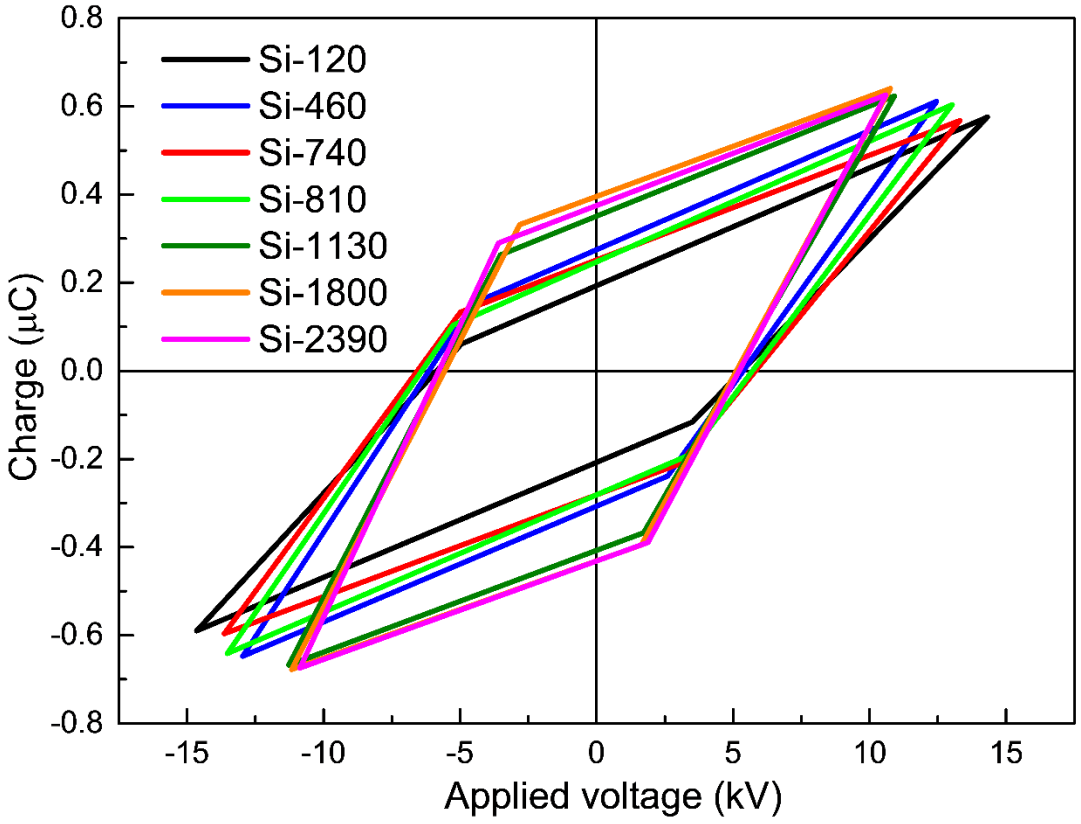

Figure S2. The slopes of Lissajous figures of plasma-based dry reforming with different particle sizes of SiO_2.

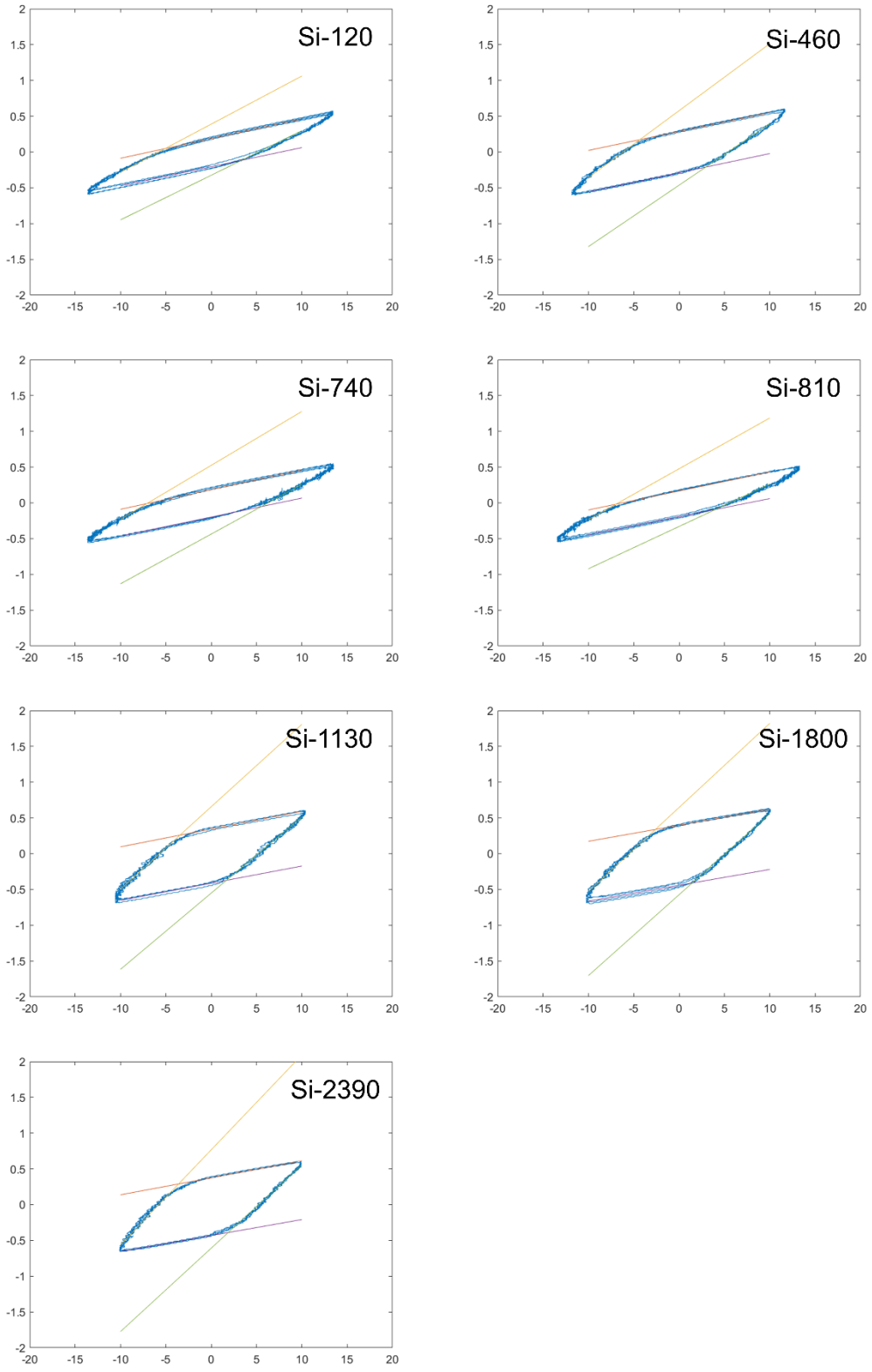

Figure S3. The raw data of Lissajous figures of plasma-based dry reforming with different particle sizes of SiO_2.

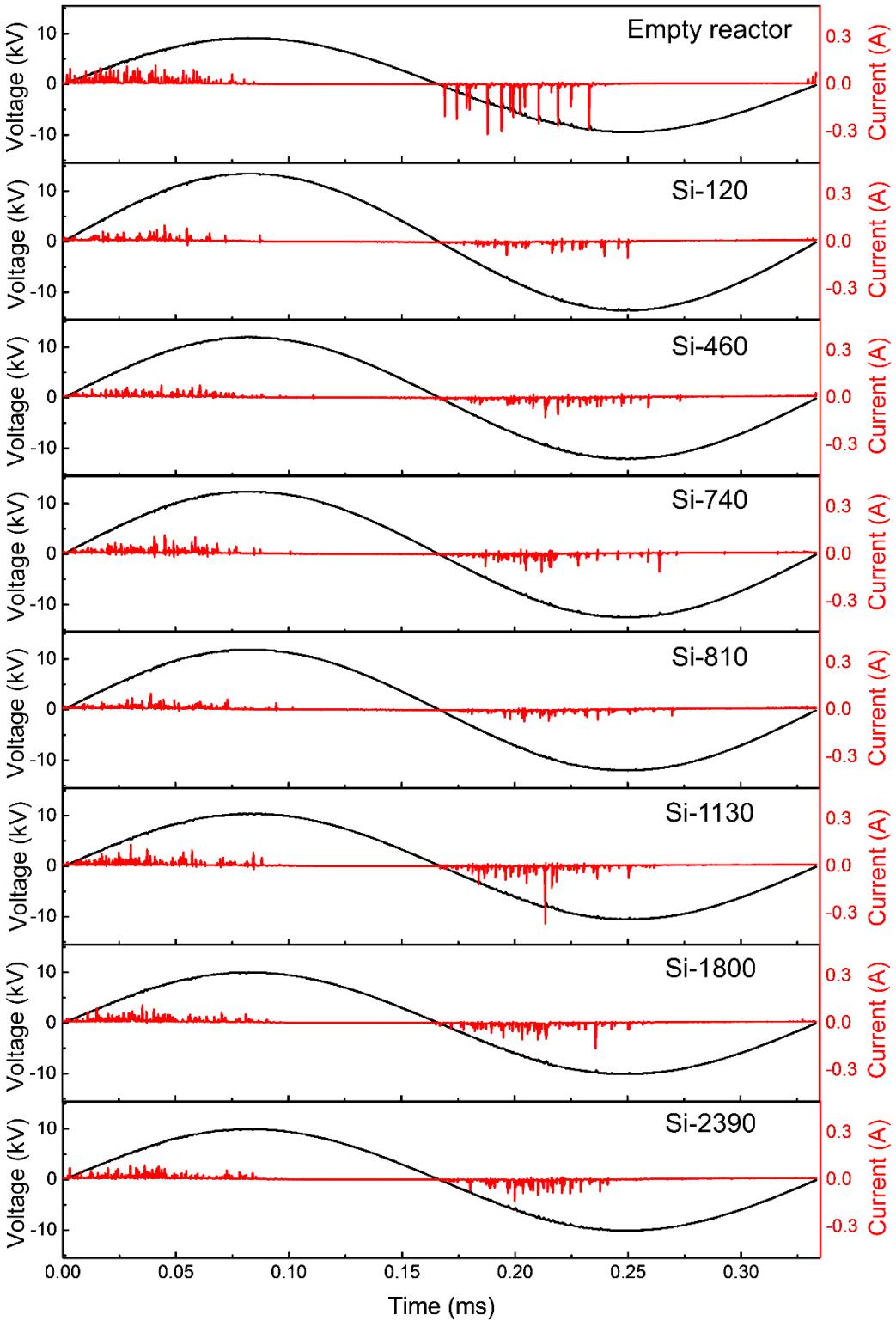

Figure S4. The raw data of voltage (black curves) and current (red curves) profiles in a period of plasma-based dry reforming with different particle sizes of SiO_2.

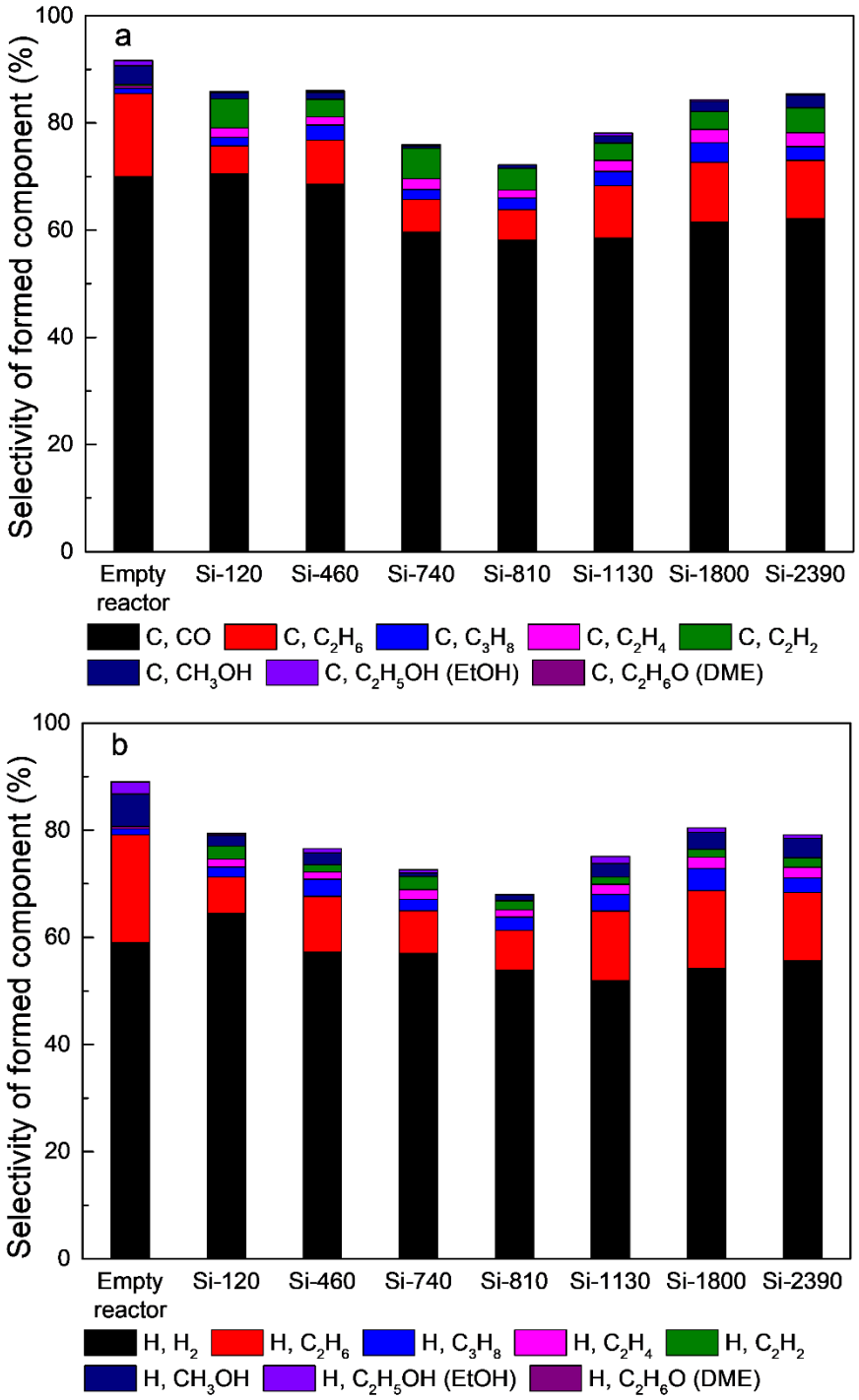

Figure S5. Product carbon-based selectivities and carbon mass balance (a) and hydrogen-based selectivities and hydrogen mass balance (b) in plasma-based dry reforming, in the empty reactor and the packed reactor with different particle sizes of SiO_2.

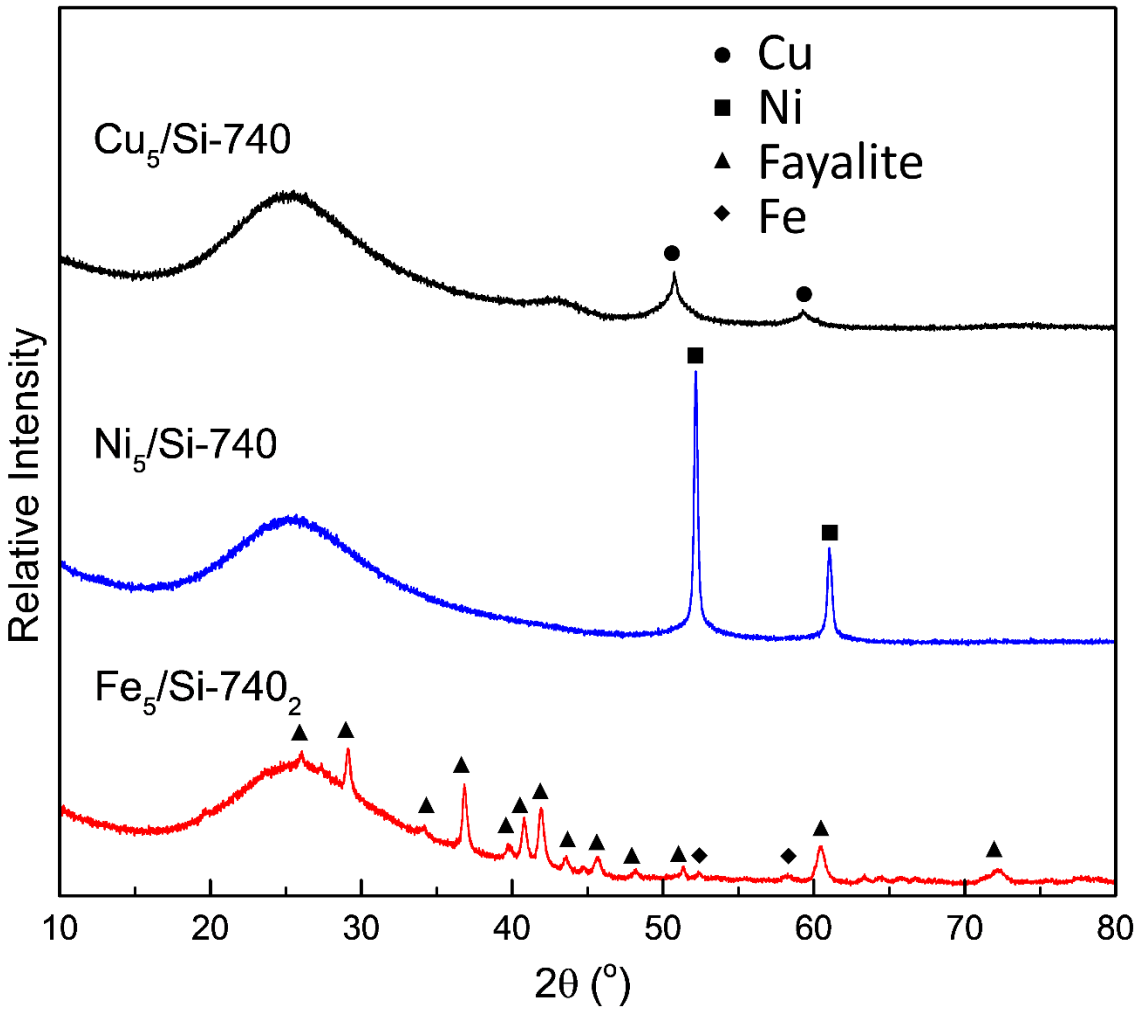

Figure S6. XRD patterns of Cu_5/Si-740, Ni_5/Si-740 and Fe_5/Si-740 after 800 ℃ reduction. Position 2θ (°) from a cobalt (Co) tube.

It can be noticed from the XRD patterns that after reduction at 800 ℃, metallic Cu and Ni supported on SiO_2 were successfully obtained, and Fe formed a fayalite solid solution with SiO_2 and a small amount of metallic Fe.

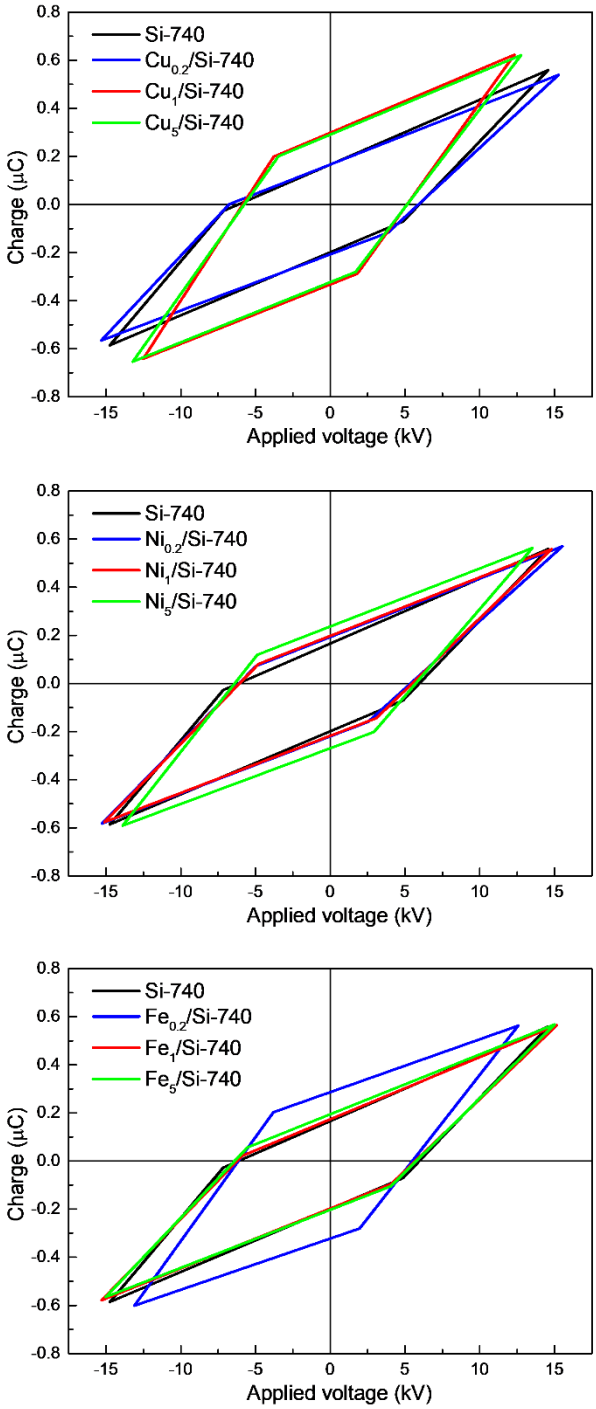

Figure S7. The slopes of Lissajous figures in plasma-based dry reforming of Si-740 with different metals and loadings.

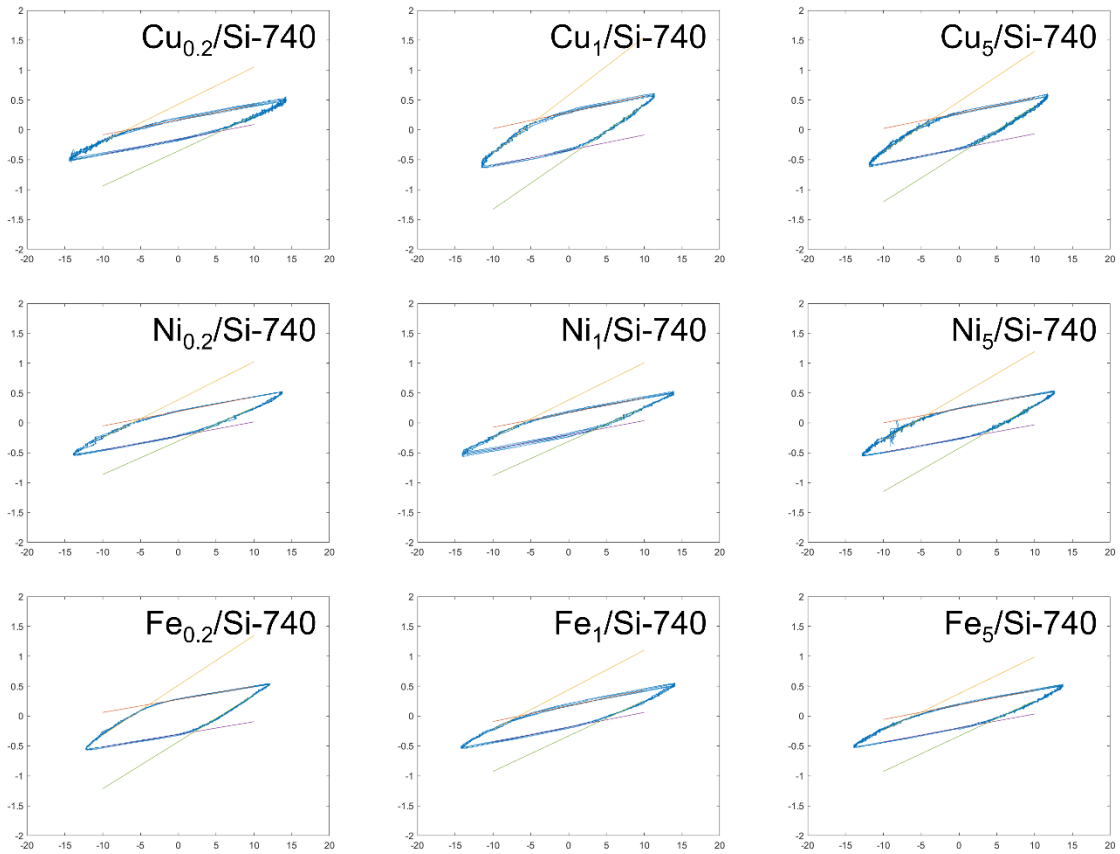

Figure S8. The raw data of Lissajous figures of plasma-based dry reforming with different particle sizes of SiO_2.

Table S1. Electrical characterization data measured and calculated from the recorded signals of the oscilloscope of the dry reforming experiments with Si-740 supporting different metals and loadings.

	Power source power (W)	Upp (kV)	Plasma power (W)	RMS Current plasma (mA)	Aver. number of μ disch. I graph	Aver. displ. Q per peak (nC/peak)
Si-740	50.31	24.84	25.95	12.45	69.81	7.67
$Cu_{0.2}$/Si-740	50.31	28.02	21.65	10.51	66.33	5.68
Cu_1/Si-740	50.50	22.76	27.21	12.78	74.29	8.52
Cu_5/Si-740	50.31	23.59	26.80	12.41	99.56	6.17
$Ni_{0.2}$/Si-740	50.89	27.67	22.66	11.01	70.25	5.88
Ni_1/Si-740	50.80	27.57	22.40	10.84	67.48	6.16
Ni_5/Si-740	50.04	25.35	24.97	11.38	79.33	6.40
$Fe_{0.2}$/Si-740	50.57	24.25	26.78	10.23	98.98	6.15
Fe_1/Si-740	50.36	27.99	21.78	9.49	67.46	5.52
Fe_5/Si-740	50.45	27.42	22.72	9.85	71.97	5.55

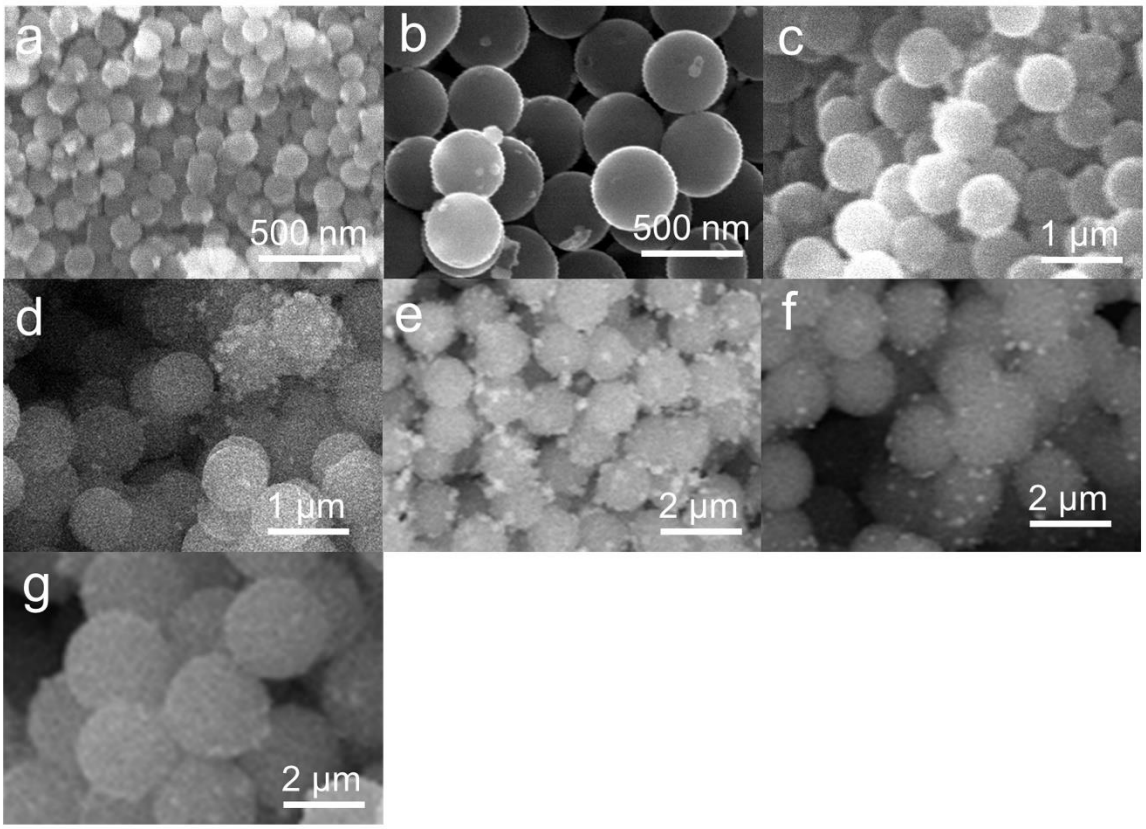

Figure S9. SEM images of impregnated and calcined (a) Ni_5/Si-120, (b) Ni_5/Si-460, (c) Ni_5/Si-740, (d) Ni_5/Si-810, (e) Ni_5/Si-1130, (f) Ni_5/Si-1800 and (g) Ni_5/Si-2390.

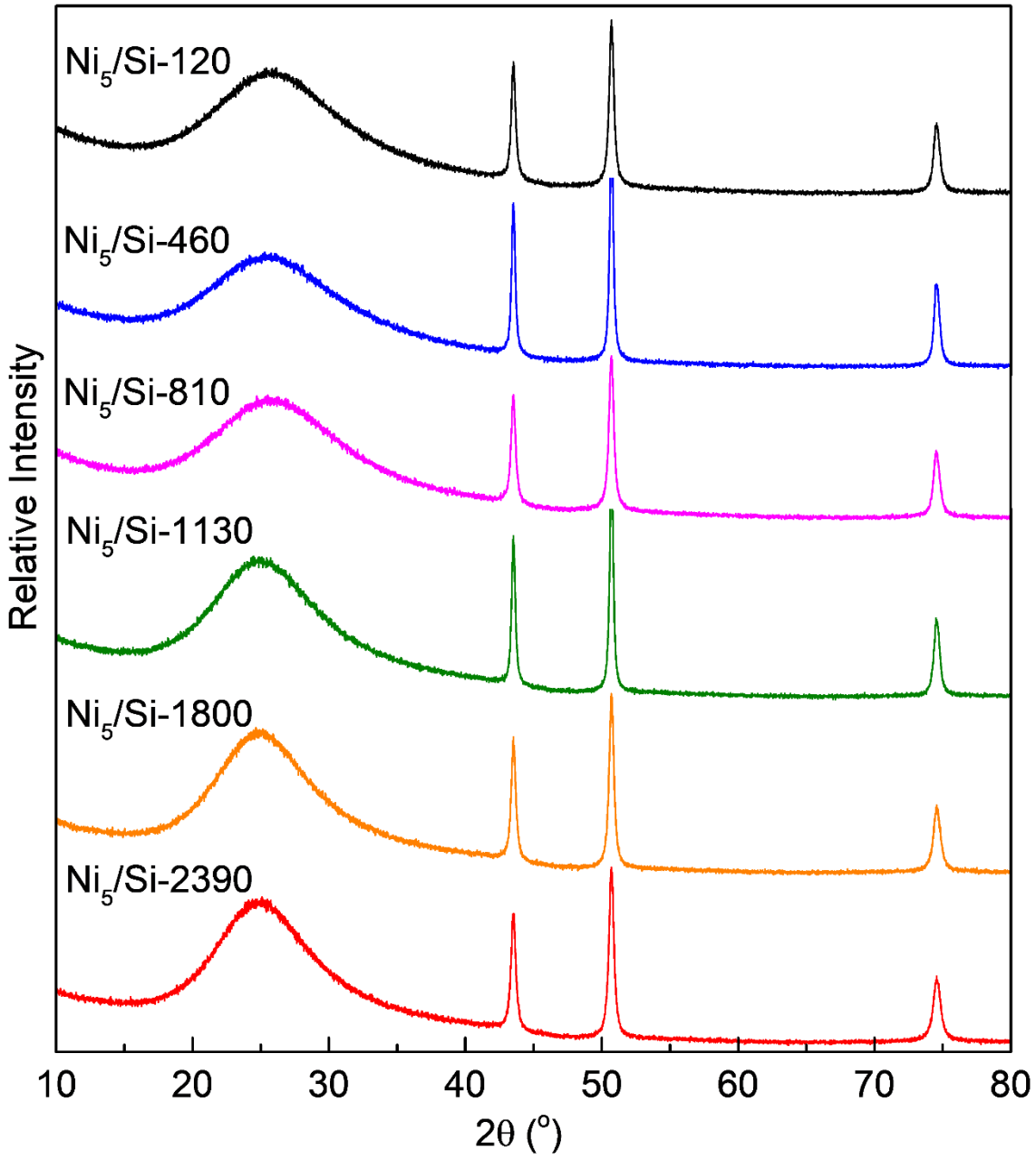

Figure S10. XRD patterns of Ni_5/Si-120, Ni_5/Si-460, Ni_5/Si-810, Ni_5/Si-1130, Ni_5/Si-1800, and Ni_5/Si-2390 after calcination at 650°C in ambient air. Position 2θ (°) from a cobalt (Co) tube.

All peaks of the XRD patterns are attribute to NiO. These samples had been reduced, but were re-calcined and then measured by XRD to compare their oxides, to prevent differences in the samples due to surface oxidation caused by storage in air.

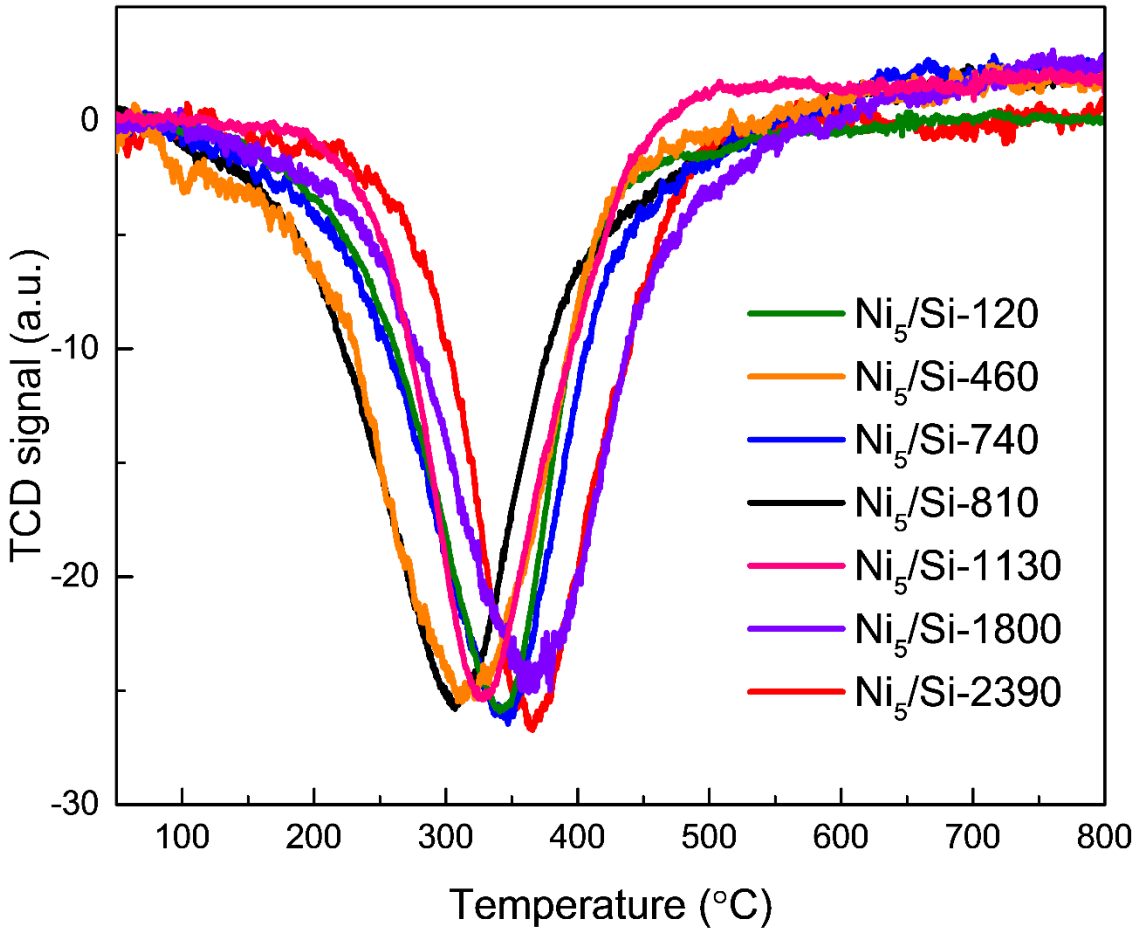

Figure S11. O_2-TPO of reduced samples (SiO_2 with different particle sizes) with 5 wt % Ni loading.

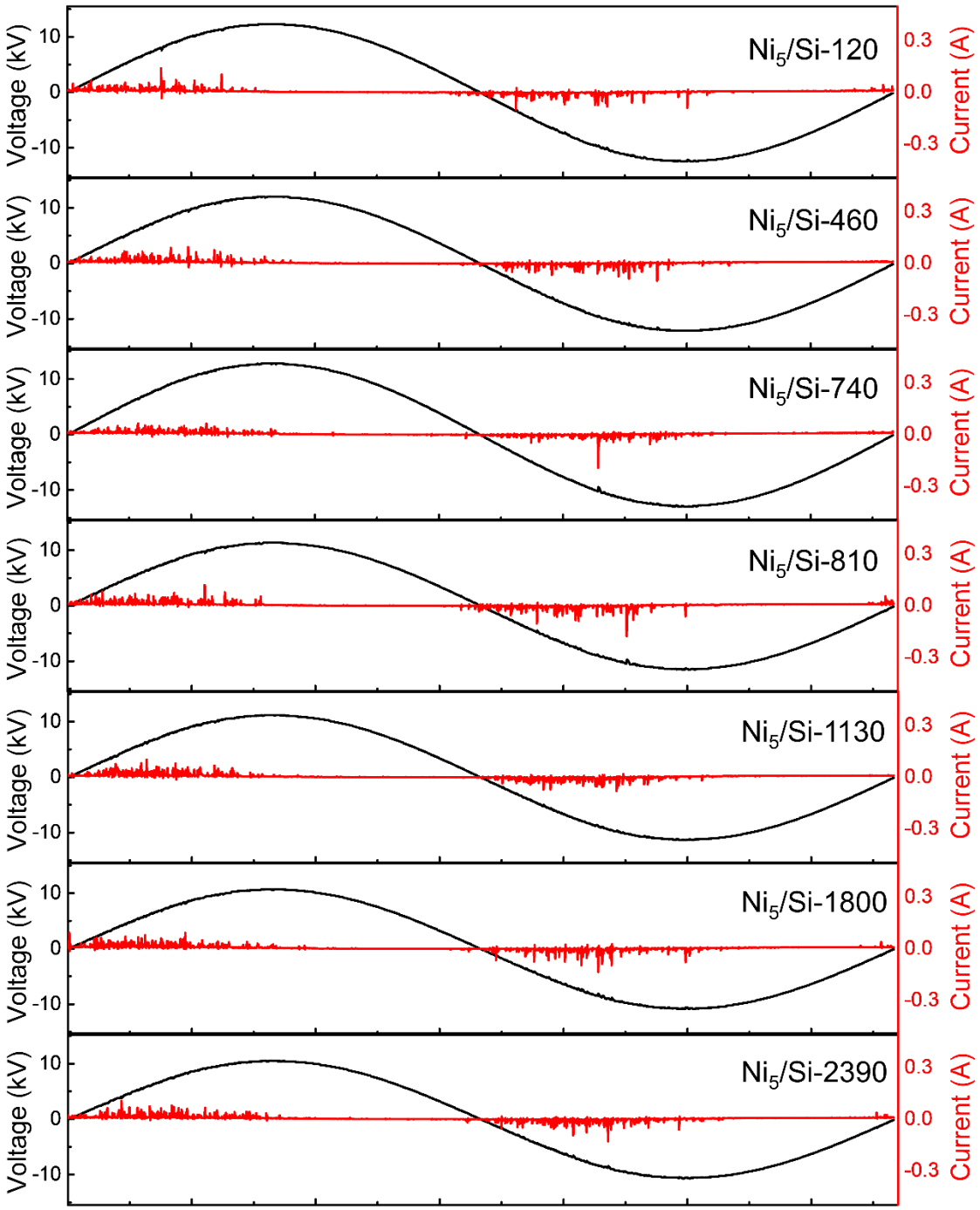

Figure S12. The raw data of voltage (black curves) and current (red curves) profiles in a period of plasma-based dry reforming with 5 wt % Ni loading on different particle sizes of SiO_2.

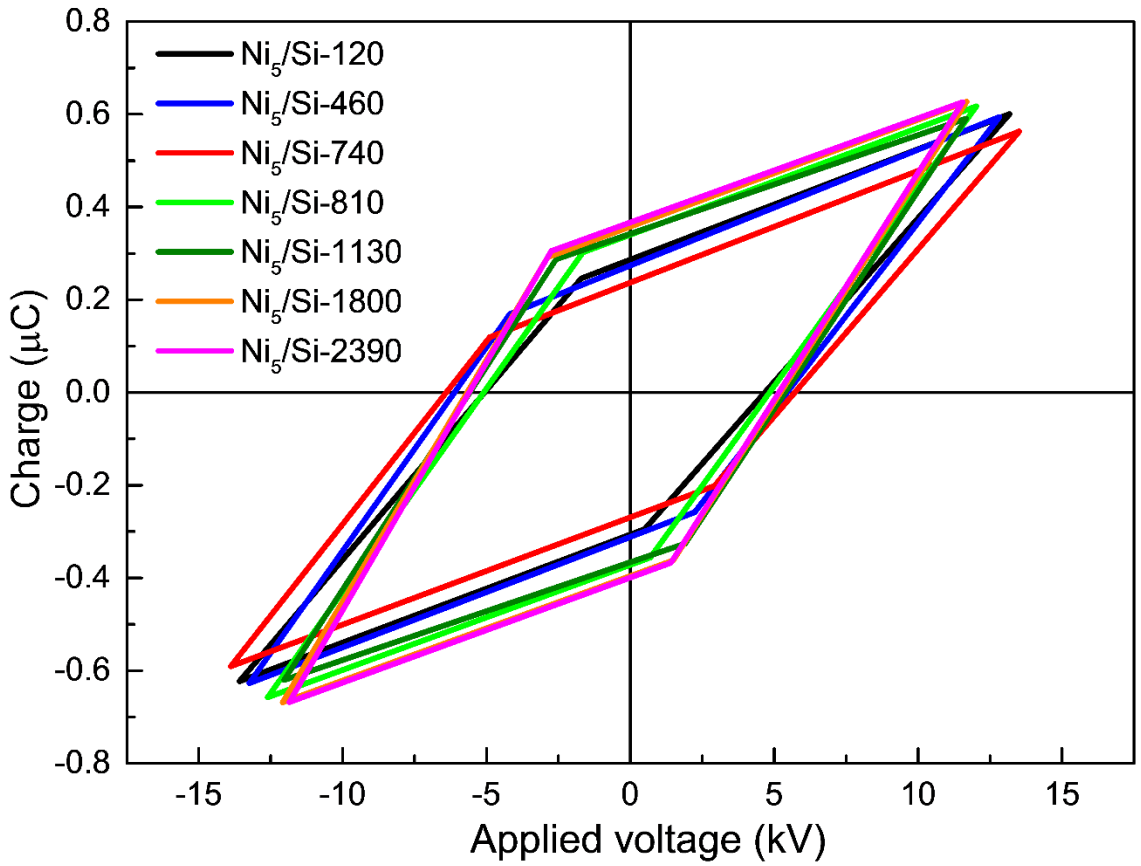

Figure S13. The slopes of Lissajous figures in plasma-based dry reforming with 5 wt % Ni loading on different particle sizes of SiO_2.

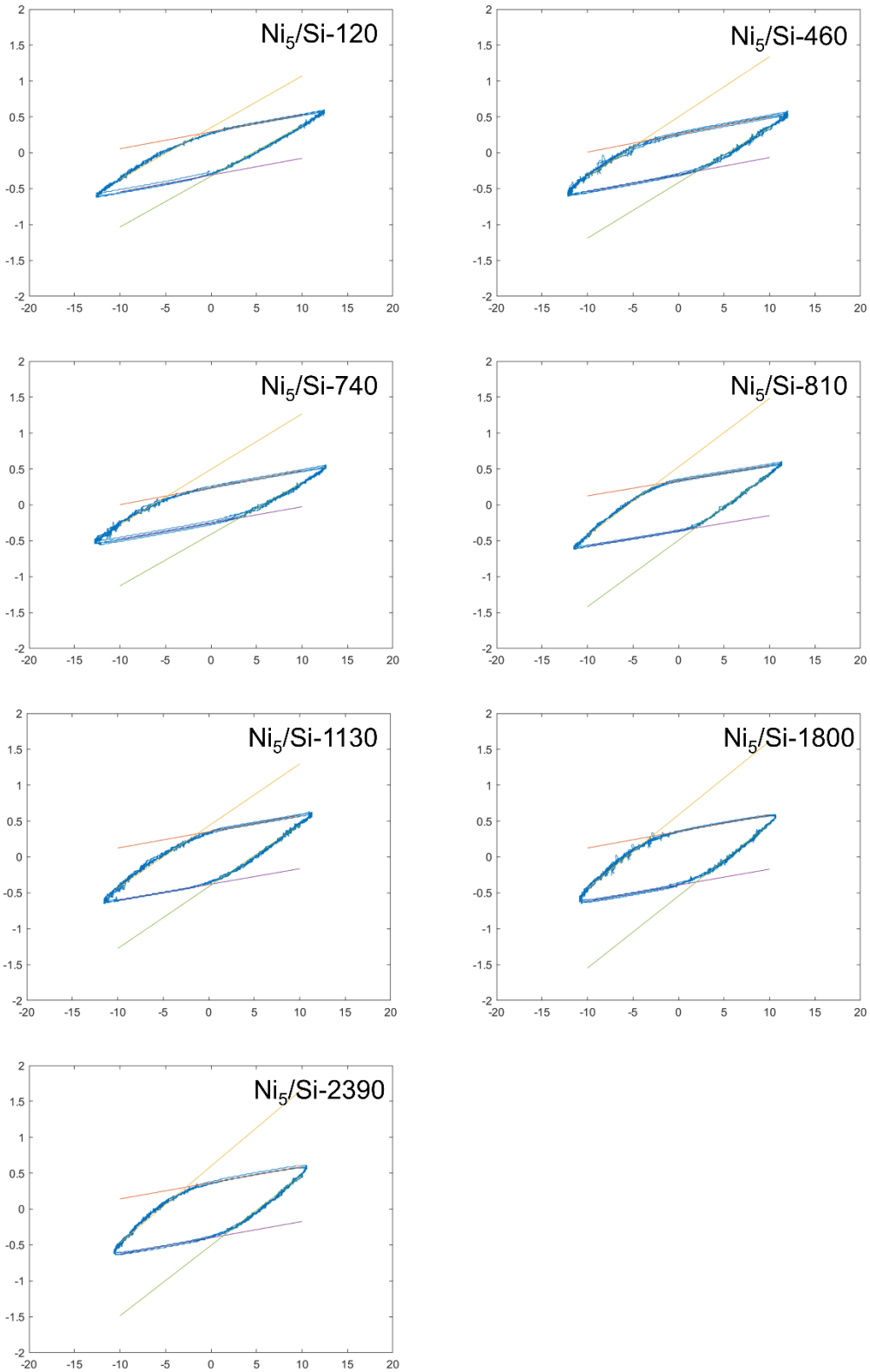

Figure S14. The raw data of Lissajous figures of plasma-based dry reforming with 5 wt % Ni loading on different particle sizes of SiO_2.

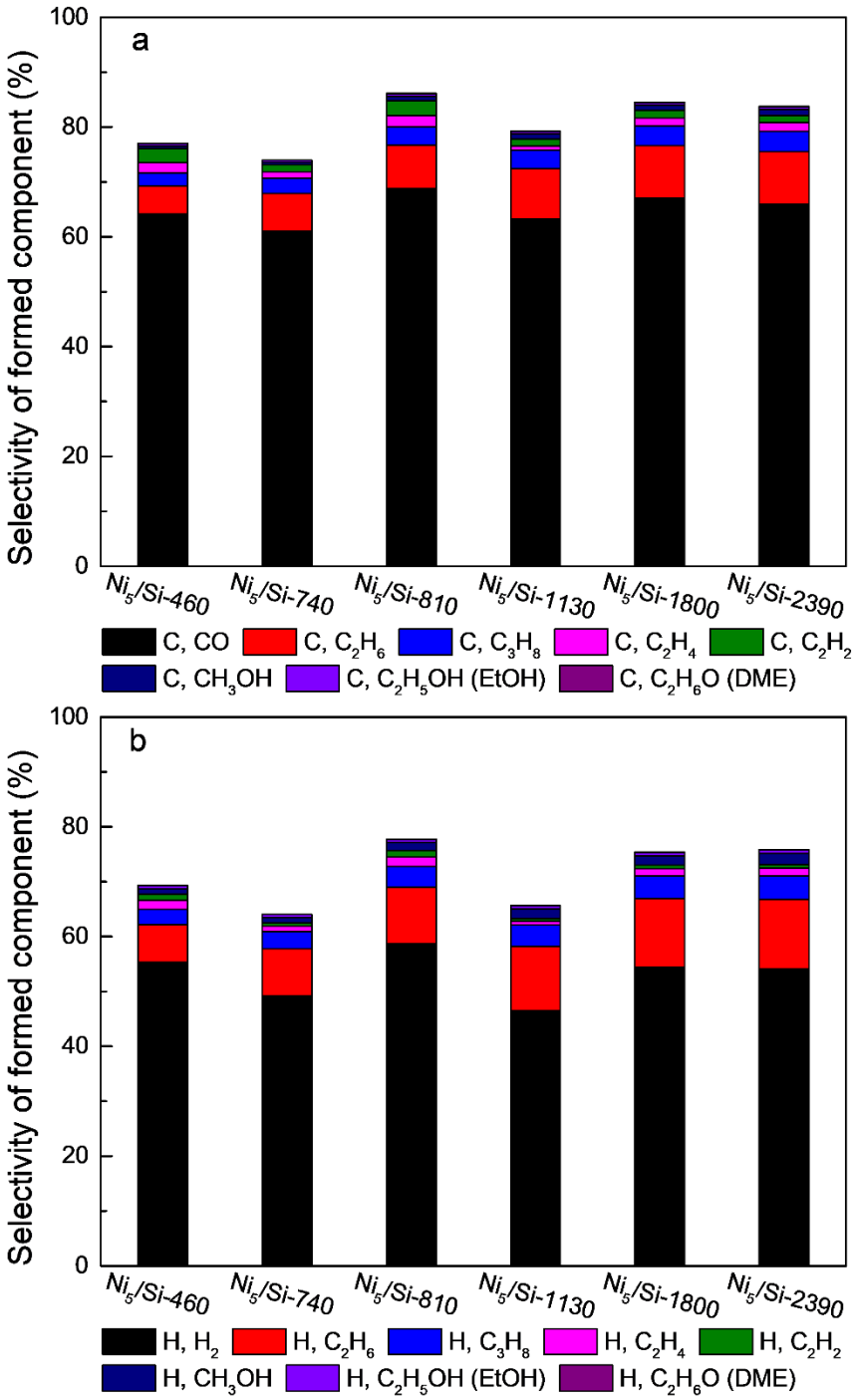

Figure S15. Product carbon-based selectivities and carbon mass balance (a) and hydrogen-based selectivities and hydrogen mass balance (b) in plasma-based dry reforming with 5 wt % Ni loading on different particle sizes of SiO_2.

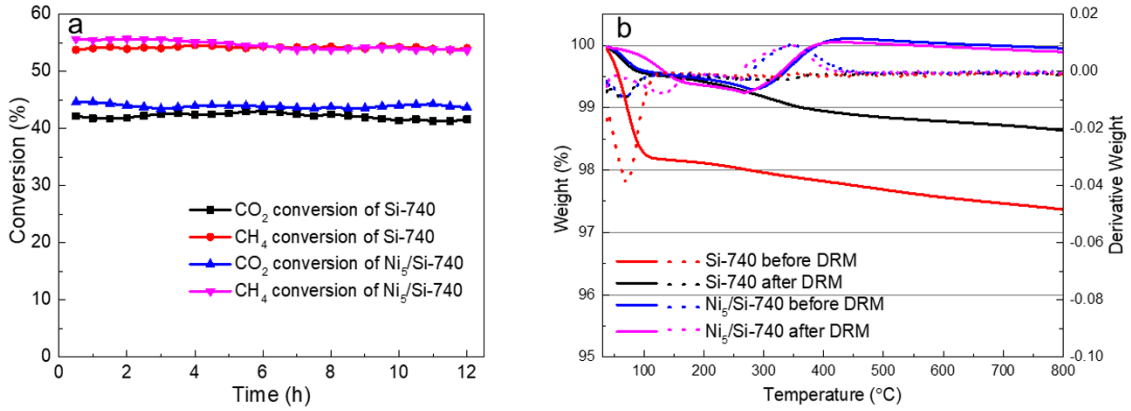

Figure S16. (a) Conversion of CH_4 and CO_2 in plasma-based dry reforming for 12 h with Si-740 and Ni_5/Si-740. (b) TGA-DTG in O_2 of Si-740 and Ni_5/Si-740 before and after DRM.